*J. Iran. Chem. Soc.*, Vol. 8, No. 1, March 2011, pp. 166-175.

JOURNAL OF THE
Iranian
Chemical Society

# Application of Multivariate Curve Resolution Analysis for Studying the Thermodynamics of Methylene Blue Aggregations in Aqueous Solutions

B. Hemmateenejad*, G. Absalan and M. Hasanpour
*Department of Chemistry, Shiraz University, Shiraz 71457, Iran*

*(Received 6 March 2010, Accepted 21 May 2010)*

In water, methylene blue (MB) is known to be aggregated to dimmer and trimmer at high concentration levels. We conducted a thermodynamic study on the aggregation of MB using multivariate curve resolution analysis of the visible absorbance spectra over a concentration range of $2.0 \times 10^{-6}$-$4.0 \times 10^{-4}$ M. A hard modeling-based multivariate curve resolution method was applied to determine the dissociation constants of the MB aggregates at various temperatures ranging from 25 to 75 °C. This method was able to resolve the visible absorbance spectra as a function of MB concentration in individual temperature or simultaneously in all other temperature ranges. Utilizing the van't Hoff relation, the enthalpy and entropy of the dissociation equilibriums were calculated. For the dissociation of both aggregates, the enthalpy and entropy changes were positive and negative, respectively.

**Keywords:** Multivariate curve resolution, Methylene blue, Aggregation, Chemometrics, Thermodynamics, Aqueous solution

## INTRODUCTION

Methylene blue (MB) (Fig. 1), one of the most commonly used thiazine dyes, is known for its pronounced metachromatic behavior and aggregation in various solutions [1,2]. The fact that the visible absorption spectra of aqueous MB solutions do not obey Beer's law has been ascribed to MB molecular aggregation [1,2], which is influenced by the concentration of the dye, the dielectric constant of the solvent, ionic strength, etc. Indeed, the MB aggregation is a complex chemical system. Numerous attempts to study this aggregation quantitatively have focused on the dimmerization [1] whereas other investigators have suggested that higher aggregates are probably formed [2].

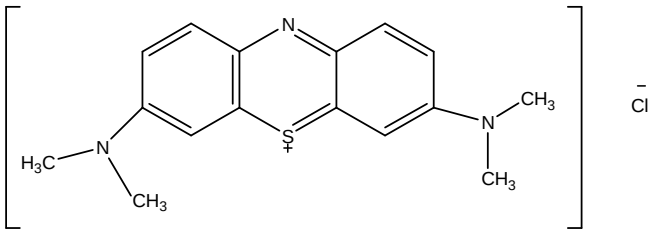


**Fig. 1.** Chemical structure of MB.

Identifying different species existing in the equilibria that cannot be isolated is one of the most challenging problems in analytical chemistry. When the compounds involved in the chemical reaction have distinct spectral responses, the analysis will be straightforward. However, in many cases, the spectral responses of two or more components overlap considerably and the analysis of their mixture can no longer be performed by classical analytical methods. On the other hand, chemometric analysis of the spectral data helps chemists to obtain analytical information from the chemical system under

*Corresponding author. E-mail: hemmatb@sums.ac.ir

Archive of SID

www.SID.ir

study [3,4]. This is accompanied by the development of instruments delivering multivariate data (such as diode array detectors, fast scanning spectrometers in the UV-Vis-NIR or Fourier transform infrared spectroscopy instruments).

Spectral curve deconvolution or multivariate curve resolution (MCR) methods are chemometric techniques concerning the extracting of the pure spectra and concentration profiles of the components in a chemical system operating in an evolutionary process [5,6]. Data analysis can be achieved by hard-modeling method where a chemical model is available or soft-modeling method where there is no robust idea about the model of the chemical reaction [5-17].

Recently, Zhao and Malinowski used a soft-modeling MCR method called windows factor analysis (WFA) to investigate the aggregation of MB in aqueous solution [18]. They detected the formation of dimmer and trimmer aggregates in the concentration interval of $1.00 \times 10^{-7}$ to $1.60 \times 10^{-2}$ M. By comparing the concentration profiles obtained from WFA calculations and solving equlibria equations, they found that the trimmer aggregate contains a chloride ion with the chemical formula of $MB_3Cl^{2+}$. Consequently, a chemical model was proposed for aggregation of MB as:

$$2MB^{+} \leftrightarrows MB_2^{2+} \quad (1)$$

$$3MB^{+} + Cl^{-} \leftrightarrows MB_3Cl^{2+} \quad (2)$$

In the present study, we used the above chemical model to study the aggregation of MB in aqueous solution. A hard modeling-based multivariate curve resolution method was applied to analyze the spectrophotometric data at different temperatures, simultaneously, by which the dissociation constants of aggregates as well as the corresponding enthalpies and entropies were calculated.

## EXPERIMENTAL

### Chemicals

All chemicals used were of analytical reagent grade. Doubly distilled water was used throughout the work. Methylene blue was purchased from Merck chemical company and was used without any further purification. Because of the acid-base character of the MB dye, all solutions were buffered with 5.0 mM phosphate buffer at pH = 7.0.

### Instrumentation

The visible absorbance spectra of the sample solutions were recorded with HP 8452A diode-array spectrophotometer with a circulated water bath thermostated at specified temperature with ±0.1 °C accuracy. Quartz cells of 1.0 and 0.1-cm path lengths were used for the diluted ($2.00 \times 10^{-6}$-$2.00 \times 10^{-5}$ M) and concentrated ($3.00 \times 10^{-5}$-$4.00 \times 10^{-4}$ M) solutions, respectively. Measurements of pH were made with a Metrohm 780 pH-meter using a combined glass electrode.

### Procedure

MB stock solutions of $1.00 \times 10^{-4}$ and $1.00 \times 10^{-3}$ M were prepared in the doubly distilled water. Then, in a series of 10.0-ml volumetric flasks desirable amounts of the stock solution was added and filled to the mark with 5.00 mM phosphate buffer solution of pH 7.0. The final analytical concentrations of MB ($[MB]_0$) in the resulting solutions were in the range of $2.00 \times 10^{-6}$-$4.00 \times 10^{-4}$ M. The visible absorbance spectra of the solutions were recorded versus buffer blank in the wavelength range of 450-750 nm and then were digitized in 2.0 nm intervals.

## DATA ANALYSIS

To compensate for the effects of variable concentrations and path lengths, an effective absorbance, similar to molar absorptivity, was calculated by dividing the absorbance data of each sample by its analytical concentration ($[MB]_0$) and path length of the cell (L):

$$A_{eff} = A/[MB]_o\, L \quad (1)$$

For each solution a row vector of the digitized absorbance values recorded at *m* wavelength was obtained and a data matrix was then provided by collecting the $A_{eff}$ row vectors of *n* solutions under each other so that the $A_{eff}$ of the most diluted and the most concentrated samples were in the first and the last rows, respectively. This data matrix is denoted by **X** sizing (*n*×*m*).

If it is assumed that monomer, $MB^{+}$, dimmer, $MB_2^{2+}$ and trimmer, $MB_3Cl^{2+}$, forms of MB are present in aqueous



Archive of SID

www.SID.ir

solutions [18], the effective absorbance of each solution at a given wavelength can be considered as the sum of contributions of all species. In matrix notation, such a relationship can be expressed as:

$$\mathbf{X} = \mathbf{CS} + \mathbf{E} \quad (2)$$

where **C** ($n\times3$) and **S** ($3\times m$) are the matrices of concentrations and spectral profiles of all methylene blue aggregates, respectively. **E** ($n\times m$) is a matrix of non-modeled absorbencies or residuals. This relationship is shown graphically in Fig. 2.

The steps taken in the employed hard-modeling method were as follows. Firstly, for the given values of dissociation constants of the aggregates (*i.e.* $K_{2d}$ and $K_{3d}$ for dimmer and trimmer, respectively), the concentration profile **C** was calculated by solving the following equilibrium expressions and mass-balance relationships:

$$(MB)_2^{2+} \leftrightarrows 2MB^+ \qquad K_{2d} = [MB^+]^2/[(MB)_2^{2+}] \quad (3)$$

$$(MB)_3Cl^{2+} \leftrightarrows 3MB^+ + Cl^- \quad K_{3d} = [MB^+]^3[Cl^-]/[(MB)_3Cl^{2+}] \quad (4)$$

$$[Cl^-] = [MB]_o - [(MB_3Cl^{2+}] \quad (5)$$

$$[MB]_o = [MB]^+ + 2[(MB)_2]^{2+} + 3[(MB)_3Cl^{2+}] \quad (6)$$

The concentration profile was the equilibrium concentrations of $[MB^+]$, $[(MB)_2^{2+}]$ and $[(MB)_3Cl^{2+}]$ species as a function of $[MB]_o$. It should be noted that since $Cl^-$ had no contribution to the absorbencies at the studied wavelength interval, its concentration was not considered in the data analysis. However, it was considered for the calculation of the trimmer dissociation constant (Eq. (4)). Each column of **C** represents the concentration profile of one of the methylene blue aggregates.

Once the concentration profile data matrix was calculated, the pure spectra data matrix was subsequently calculated by least square solution of Eq. (2) [19]:

$$\mathbf{S} = \mathbf{C}^+\mathbf{X} \quad (7)$$

where the superscript "$^+$" denotes pseudo-inverse of a matrix.

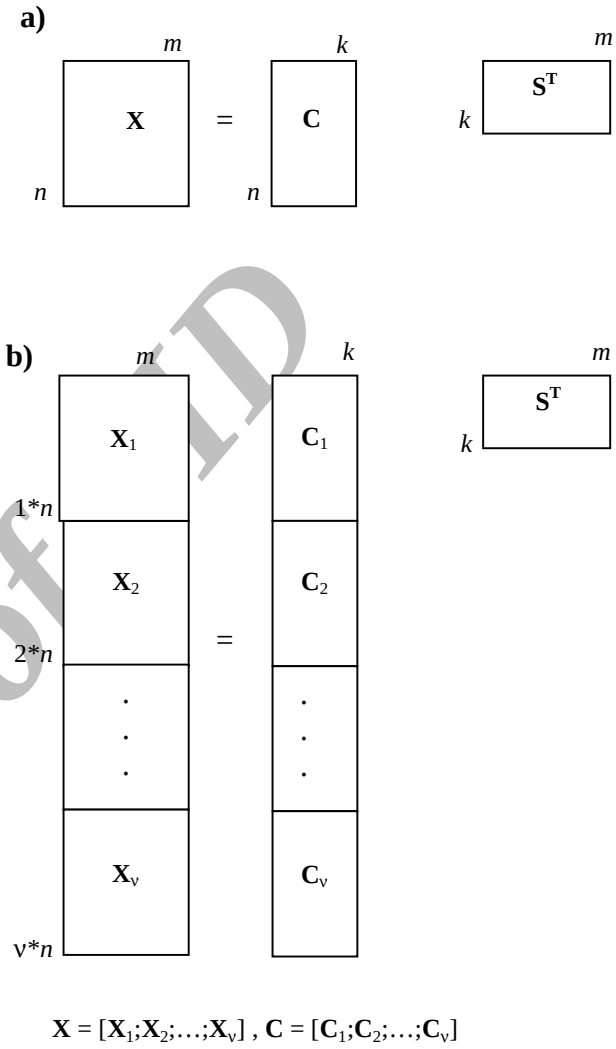


$\mathbf{X} = [\mathbf{X}_1;\mathbf{X}_2;\ldots;\mathbf{X}_v]$ , $\mathbf{C} = [\mathbf{C}_1;\mathbf{C}_2;\ldots;\mathbf{C}_v]$

**Fig. 2.** Graphical representation of data matrix arrays in the multivariate curve resolution analysis of (**a**), a single aggregation process and (**b**), simultaneous analysis of several experiments at different temperatures: **X**i is the absorbance data matrix of the aggregation process recorded at the $i^{th}$ temperature, **C**i is the concentration profile of MB aggregates at the $i^{th}$ temperature and **S** is the matrix of pure spectra of the MB aggregates. The superscript "$^T$" denotes the matrix transpose.

Since negative absorbance values were meaningless, a non-negativity constraint was thus implemented by forcing the negative elements of **S** to zero. Once **C** and **S** matrices were



Archive of SID

www.SID.ir

calculated, the rebuilt absorbance data matrix ($\hat{\mathbf{X}}$) is calculated by post-multiplication of **C** by **S** (Eq. (2)).

The calculated concentration and spectral profiles are evaluated by calculating the least squares error function ($\chi^2$) [20], which is the difference between the original ($x_{i,j}$) and the predicted ($\hat{x}_{i,j}$) data, weighted by the inverse of the number of degrees of freedom in the fit:

$$\chi^2 = \frac{\sum_{i=1}^{m}\sum_{j=1}^{n}(\hat{x}_{i,j} - x_{i,j})^2}{(m*n) - [(k*n) + (p*k)]} \quad (8)$$

In the above equation, *p* is the number of unknown parameters for a single profile (here $K_{2d}$ and $K_{3d}$), *m* and *n* are the number of rows and columns in **X**, and *k* is the number of chemical species considered in the model (here 3 species $MB^+$, $(MB)_2^{2+}$ and $(MB)_3Cl^{2+}$). Because negative intensities in **S** had no physical meaning, an additional penalty was added to $\chi^2$ to help the search converge quickly. The objective function $\overline{\chi}^2$ with the penalty term is defined as [21]:

$$\overline{\chi}^2 = \chi^2\left(1 + 10\frac{\sum_{i=1}^{n}\sum_{j=1}^{k}|s_{i,j} < 0|}{\sum_{i=1}^{n}\sum_{j=1}^{k}|si,j|}\right) \quad (9)$$

This objective function considers the fraction of negative elements of **S** (*i.e.*, $s_{i,j} < 0$) as optimization criterion in addition to the difference between the calculated and measured absorbencies. It should be noted that negative values were indicated before the implementation of non-negativity to spectral profiles. Thus, this function tends to minimize both residual error and fraction of negative elements of **S**. The "fminsearch" function implemented in MATLAB was applied to minimize the objective function $\overline{\chi}^2$ by changing the equilibrium dissociation constants $K_{2d}$ and $K_{3d}$. Fminsearch is a nonlinear optimization function, which is also known as a direct method, because it does not use numerical or analytical gradients. It finds the minimum of a function by optimizing several variables with an initial guess; lower and upper bounds are not required. It uses the simplex optimization algorithm of Nelder-Meader [22]. The output of this method is the optimum values of $K_{2d}$ and $K_{3d}$, at which the objective function $\overline{\chi}^2$ is at its lowest value.

The aforementioned hard-modeling method can be extended to analyze the absorbance data of several experiments (*i.e.* aggregation at several temperatures), simultaneously [23]. Such arrays of data are shown in Fig. 2b. The **X** and **C** matrices are augmented ones formed by staking those of each experiment on the top of each other. Assuming that the pure spectra and nature of the species were independent of temperature, there would be only one pure spectra data matrix (**S**) for all the examined temperatures. However, since equilibrium constants are dependent on temperature, different concentration profiles were calculated for each temperature. Therefore, at each temperature a separate pair of $K_{2d}$ and $K_{3d}$ was used to describe the changes in the concentration of the MB species as the function of initial concentration. In this case, the objective function $\overline{\chi}^2$ was dependent on the equilibrium constants at all temperatures. If the experiment was conducted at ν different temperatures, ν pairs of equilibrium constants must have been varied by "fminsearch" algorithm to obtain the lowest value of $\overline{\chi}^2$. Here, the aggregation of MB was studied at temperatures 25, 35, 45, 55, 65 and 75 °C. Thus, for the simultaneous analysis of the absorbance data, 12 equilibrium constants were varied to obtain the optimum objective function $\overline{\chi}^2$.

## RESULT AND DISCUSSION

The changes in the effective absorptivity of MB as a function of the analytical concentration of the indicator at three different temperatures (*i.e.*, 25, 45 and 65 °C) are given in Fig. 3. As can be seen, the absorbance spectrum of the most diluted MB solution, in which MB is mainly present as monomeric species, is composed of a narrow band and a shoulder at 660 and 610 nm, respectively. As the concentration of MB is increased, the band at 610 nm is first increased and then decreased at analytical MB concentrations higher than $1.00 \times 10^{-4}$ M. The changes are accompanied with the disappearance of the band at 660 nm. These spectral changes are the evidence for the presence of two or more forms of MB in the solutions. Similar results were obtained for temperatures at 25, 35, 55, 65 and 75 °C. Zhao and Malinowski [18] have proposed a two-step aggregation for MB upon increasing the initial concentration of the indicator. The factor analysis of the effective absorbance data at all the



Archive of SID

www.SID.ir

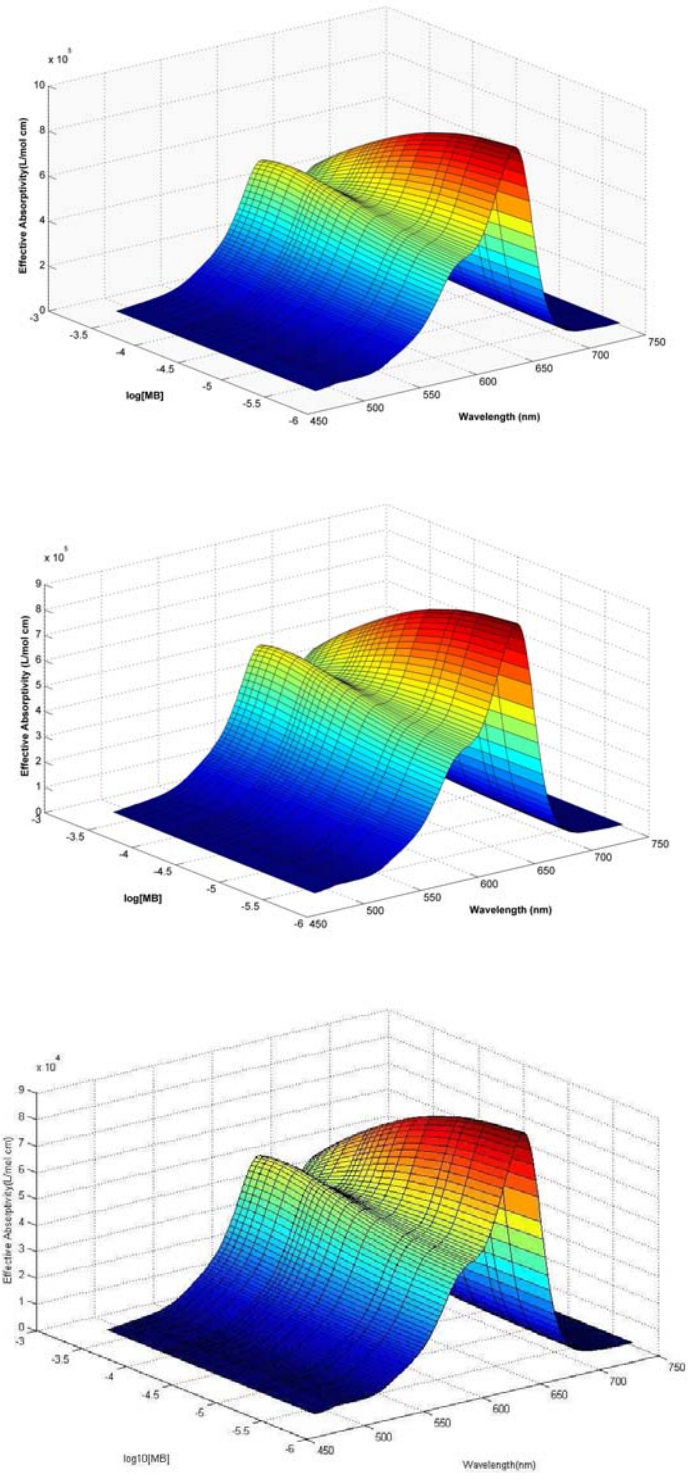


**Fig. 3.** Three-dimensional plot of effective absorptivity spectra of aqueous MB solutions with concentrations ranging from $2.00 \times 10^{-6}$ to $4.00 \times 10^{-4}$ M at three representative temperatures.



www.SID.ir

**Table 1.** The Results of Application of Factor Analysis (Logarithm of Eigen-Values) on the Effective Absorptivity Data Matrices of Various Temperatures

| No. of factors | 25 °C | 35 °C | 45 °C | 55 °C | 65 °C | 75 °C |
|---|---|---|---|---|---|---|
| 1 | 12.42 | 12.43 | 12.44 | 12.45 | 12.45 | 12.46 |
| 2 | 10.47 | 10.48 | 10.46 | 10.45 | 10.44 | 10.43 |
| 3 | 7.75 | 7.76 | 7.65 | 7.60 | 7.57 | 7.56 |
| 4 | -5.72 | -5.69 | -5.66 | -5.62 | -5.68 | -5.64 |
| 5 | -6.49 | -6.48 | -6.46 | -6.54 | -6.51 | -6.41 |
| 6 | -6.88 | -6.83 | -6.84 | -6.81 | -6.76 | -6.84 |

studied temperatures (Table 1) revealed the presence of three chemical species coexisting in the aggregation process of MB. In addition, three components were identified by factor analysis of the augmented data matrices. These detected species can be related to monomer, dimmer and trimmer forms of MB. According to the finding of Zhao and Malinowski [18], we considered one $Cl^-$ ion in the trimmer form of MB.

The recorded effective absorbance data through MB aggregation process were first analyzed by the explained hard-model method at each temperature separately. The resulting concentration profiles showed the lower stability of trimmer and dimmer at higher temperatures. This can be attributed to the weakening of MB-MB interactions in the aggregates by increasing temperature. However, we could not rely on the estimated dissociation constants of the aggregates since we observed some differences between the resolved pure absorbance spectra of the species at different temperatures. Thus, the data were subjected to simultaneous hard-modeling analysis to obtain unique pure absorbance spectra for each species at all studied temperatures.

The resolved spectral profiles of the different MB aggregates, after convergence of the simultaneous hard-modeling analysis of the absorbance-concentration data at various temperatures, are presented in Fig. 4. There was a very strong similarity between the resolved pure spectrum of MB monomer and that recorded for the most diluted MB solution, which contains mainly monomer species. The monomer pure spectrum possesses a narrow peak at 660 nm and a shoulder at 610 nm. The ratio of peak intensity at these wavelengths is reversed for dimmer compared with that of monomer. The

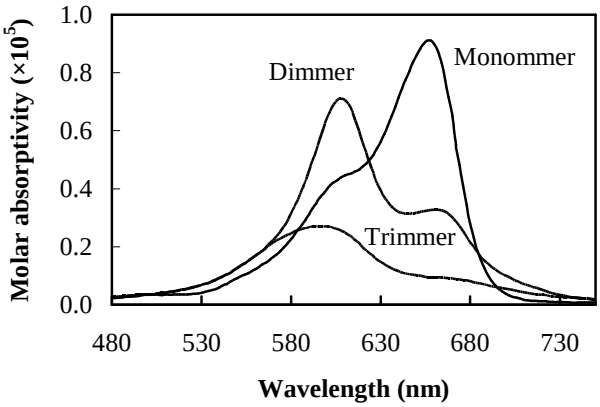


**Fig. 4.** The resolved pure spectra of different MB aggregates.

shoulder of the monomer pure spectrum at 610 nm changed to a clear narrow peak for dimmeric form of MB. On the other hand, the dimmer pure spectrum exhibited a weaker and broader peak at about 660 nm with a small blue shift compared to that of monomer. Moreover, the pure spectrum of dimmer showed a weak shoulder at about 700 nm while this was not observed for that of monomer. The pure spectrum of trimmer was similar to that of dimmer. However, it had lower intensity and the peak of dimmer at about 660 nm changed to a flat and broad shoulder in trimmer.

The resolved concentration profiles at different temperatures are given in Fig. 5 and the calculated dissociation constants associated with these concentration profiles are listed in Table 2. It is observed that in the most diluted solution (*i.e.*, $2.00 \times 10^{-6}$ M), MB mainly exists as monomer



Archive of SID

www.SID.ir

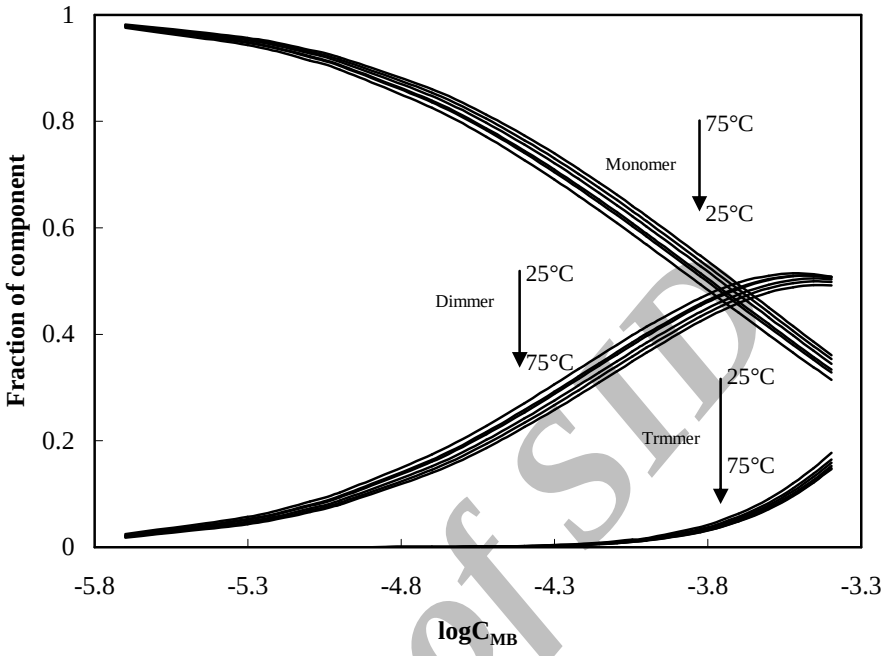


**Fig. 5.** Concentration profiles of different MB aggregates as function of the logarithm of analytical concentration of MB ($logC_{MB}$) at different studied temperatures.

**Table 2.** The Calculated Dissociation Constant of Dimmer ($k_{2d}$) and Trimmer ($k_{3d}$) Aggregates of Methylene Blue in Water at Different Temperature

| T ($^oC$) | $k_{2d}$ | $k_{3d}$ |
|---|---|---|
| 25 | $1.56 \times 10^{-4}$ | $3.18 \times 10^{-11}$ |
| 35 | $1.70 \times 10^{-4}$ | $3.88 \times 10^{-11}$ |
| 45 | $1.75 \times 10^{-4}$ | $4.25 \times 10^{-11}$ |
| 55 | $1.89 \times 10^{-4}$ | $4.90 \times 10^{-11}$ |
| 65 | $2.00 \times 10^{-4}$ | $5.40 \times 10^{-11}$ |
| 75 | $2.12 \times 10^{-4}$ | $5.85 \times 10^{-11}$ |

and upon increasing the analytical concentration of MB, the dimmeric form is evolved accompanied with a decrease in the amount of monomer. At analytical concentration of about $2.00 \times 10^{-5}$ M, the trimmer aggregate begins to evolve. Below this concentration limit, only monomer and dimmer are in equilibrium whereas in the more concentrated solutions, all MB species are in equilibrium.

A comparison between the concentration profiles at different temperatures reveals that an increase in temperature destabilizes the dimmer and trimmer aggregates. Consequently, the mole fractions of these aggregated species are decreased by increasing the temperature. These observations are in agreement with the calculated dissociation constants. As it is shown in Table 2, the dissociation constants of both dimmer and trimmer are increased by increasing the temperature. These findings suggest that for an aqueous MB



Archive of SID

www.SID.ir

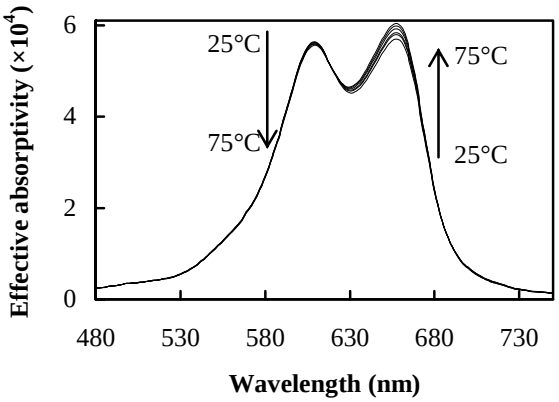


**Fig. 6.** Effective absorptivity of $1.00 \times 10^{-4}$ M MB solution at temperatures of 25 °C to 75 °C in 10 °C intervals.

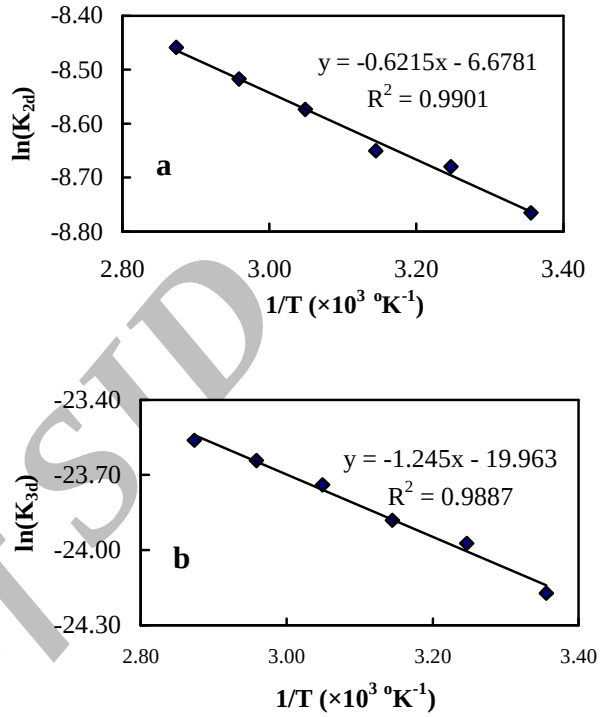


**Fig. 7.** The plots of logarithm of dissociation constants ($k_{2d}$ and $k_{3d}$) against the inverse of temperature Kelvin (van't Hoff ) for the dissociation of MB aggregates: a) dimmer and b) trimmer.

solution with a given analytical concentration, the relative amounts of monomer, dimmer and trimmer are changed by changing the temperature so that an increase in temperature decreases the concentration of dimmer and trimmer, which is accompanied with an increase in the concentration of monomer.

The changes in absorbance spectra of $2.00 \times 10^{-4}$ M solution of MB as a function of temperature are shown in Fig. 6. An increase in absorbance at 660 nm and a decrease in absorbance at 610 nm are observed upon increasing the temperature. This confirms the shift of equilibrium toward the dissociation of aggregates and increasing the concentration of monomer as it has higher molar absorptivity at 660 nm and a lower one at 610 nm.

The estimated equilibrium constants at different temperatures can be used to calculate the thermodynamic parameters of the dissociation processes. If the standard enthalpy and entropy changes of a reaction (ΔH° and ΔS°, respectively) are not strongly dependent on the temperature,van't Hoff equation can be used to describe the relationship between equilibrium constant and temperature:

$$\ln K = -(\Delta H^\circ/RT) + \Delta S^\circ/R \qquad (10)$$

where R is the gases constant and T is temperature in K. As it is shown in Fig. 7, there is a well-defined linear relationship between the logarithm of dissociation constant and inverse of Kelvin temperature. The slope and intercept of the plots were used to calculate the standard enthalpy and entropy changes of dissociations, respectively. The results are given in Table 3. For both dissociation reactions, the enthalpy change is positive, which means that dissociation of aggregates to monomer is endothermic. On the other hand, the entropy change of dissociations is negative, which means that by dissociation of dimmers or trimmers to their monomer molecules the entropy of the system is decreased. This may seem to be surprising since, through dissociation, the number of MB molecules in the products is larger than that of reactants. However, since we studied the system in aqueous solution, the relative number of solvent molecules surrounding the monomers and aggregates should be considered as well. Hydrophobic interaction is the main reason for aggregation of organic dye monomers in aqueous solutions. At high concentrations, the hydrophobic molecules are released from



Archive of SID

www.SID.ir

**Table 3.** The Calculated Standard Enthalpy and Entropy Changes of Dissociation Reactions (ΔH° and ΔS°, Respectively) of MB Aggregates

| Aggregate | ΔH° (J $mol^{-1}$) | ΔS° (J $mol^{-1}$ $K^{-1}$) |
|---|---|---|
| Dimmer | 5172 | -56 |
| Trimmer | 10360 | -166 |

the solvent cage through aggregation, by which some solvent molecules bonded to the monomers are liberated. This phenomenon can be shown as the following chemical equation:

$$n[MB(H_2O)_m] \leftrightarrows [(MB)_n(H_2O)_q] + (n\times m-q)\ H_2O \qquad (11)$$

where n is aggregation number and m and q are the number of water molecules surrounding the monomer and aggregate molecules, respectively. Equation (11) shows that some water molecules are released in the dissociation process. If the number of released water molecules (*i.e.*, n×m-q) is higher than n-1 (difference between the number of monomer and aggregate molecules), the entropy of the system is increased by aggregation. According to the above discussion, the negative values of entropy change for aggregate dissociation indicate that some water molecules are consumed through dissociation. In other words, some water molecules are liberated through aggregation.

## CONCLUSIONS

This research dealt with the application of chemometric methods for spectrophotometric study of the thermodynamics of aggregation of methylene blue in aqueous solution. By simultaneous analysis of the absorbance data recorded at various analytical concentrations of the dye and various temperatures, it was possible to calculate the dissociation constants of the trimmer and dimmer forms and consequently to calculate enthalpy and entropy changes of the reactions. It was found that both dissociation reactions are endothermic and therefore an increase in temperature destabilizes the aggregates. The entropy change was found to be negative, which means that the monomeric state of the dye is more structured compared to the aggregates. This was attributed to the higher solvation of monomer molecules relative to aggregates.

## ACKNOWLEDGEMENTS

Financial support of this project by the Research Council of Shiraz University is highly appreciated.

## REFERENCES

[1] K. Bergmann, C.T. O'Konski, J. Phys. Chem. 67 (1963) 2169.
[2] E. Braswell, J. Phys. Chem. 72 (1967) 2477.
[3] B. Lavine, J. Workman, Anal. Chem. 80 (2008) 4519.
[4] B. Hemmateenejad, Chemometr. Intell. Lab. Syst. 81 (2006) 202.
[5] A. de Juan, R. Tauler, Crit. Rev. Anal. Chem. 36 (2006) 163.
[6] E.R. Malinowski, Factor Analysis in Chemistry, Wiley-VCH, Weinheim, 2002.
[7] R. Rajko, J. Chemometr. 23 (2009) 172.
[8] B. Hemmateenejad, K. Javidnia, M. Saeidi-Boroujeni, J. Pharm. Biomed. Anal. 47 (2008) 625.
[9] H. Abdollahi, M. Maeder, R. Tauler, Anal. Chem. 81 (2009) 2115.
[10] B. Hemmateenejad, M.R.H. Nezhad, J. Phys. Chem. C 112 (2008) 18321.
[11] L. Chen, Chemometr. Intell. Lab. Syst. 94 (2008) 123.
[12] B. Hemmateenejad, J. Chemom. 19 (2005) 657.
[13] M. Shamsipur, B. Hemmateenejad, A. Babaei, L. Faraj-Sharabiani, J. Electroanal. Chem. 570 (2004) 227.
[14] M. Maeder, A.D. Zuberbuhler, Anal. Chem. 62 (1990) 2220.
[15] L. Antonov, D. Nedeltcheva, Chem. Soc. Rev. 29 (2000) 217.



Archive of SID

www.SID.ir

[16] J. Blobel, P. Bernadó, D.I. Svergun, R. Tauler, M. Pons, J. Am. Chem. Soc. 131 (2009) 4378.
[17] M. Shamsipur, B. Hemmateenejad, M. Akhond, K. Javidnia, R. Miri, J. Pharm. Biomed. Anal. 31 (2003) 1013.
[18] Z. Zhao, E.R. Malinowski, J. Chemometr. 13 (1999) 83.
[19] R. Tauler, A.K. Smilde, B.R. Kowalski, J. Chemometr. 9 (1995) 31.
[20] S.D. Frans, M.L. McConnell, J.M. Harris, Anal. Chem. 57 (1985) 1552.
[21] M. Wasim, R.G. Brereton, J. Chem. Inf. Model. 46 (2006) 1143.
[22] S.L. Morgan, S.N. Deming, Anal. Chem. 46 (1974) 1170.
[23] C. Ruckebusch, A. de Juan, L. Duponchel, J.P. Huvenne, Chemometr. Intell. Lab. Syst. 80 (2006) 209.

of SID



www.SID.ir